INTERNATIONAL JOURNAL OF CONSERVATION SCIENCE

ISSN: 2067-533X Volume 8, Issue 1, January-March 2017: 59-66 www.ijcs.uaic.ro

MULTIVARIATE ANALYSES OF SOLUBLE SALTS RESPONSIBLE FOR PATHOLOGIES IN GRANITES OF THE ROMAN AQUEDUCT OF SEGOVIA, SPAIN

Adolfo Carlos INIGO[1*], Jacinta GARCÍA-TALEGÓN[2], Santiago VICENTE-TAVERA[3], Soledad CASADO-MARÍN[1], Sara MARTÍN-GONZÁLEZ[1]

[1] Instituto de Recursos Naturales y Agrobiología de Salamanca (IRNASA-CSIC), c) Cordel de Merinas 40-52, 37008 Salamanca.
[2] Departamento de Geología, Universidad de Salamanca, Spain.
[3] Departamento de Estadística, Universidad de Salamanca, Spain.

Abstract

The aim of this work is to characterize the main pathologies caused by salt crystallization in granitic monuments (crusts, salt efflorescence, disaggregation and disaggregation with salt efflorescence). Water soluble ions were determined quantitatively. Using the Canonical Biplot multivariate method it was determined that: a) there is a relationship between the content of water soluble salts and the different identified pathologies; b) sulphate and NO_3^-, Cl^-, Ca^{2+}, Mg^{2+}, K^+ and Na^+ ions are the major components of salt efflorescence; c) carbonate is a major component of the crust; and d) the disaggregated granites, with or without salt efflorescence, have a low proportion of soluble salts but no predominant ion composition.

Keywords: *Granite; Pathologies; Salt crystallization; Crust; Efflorescence; Disaggregation; Canonical Biplot*

Introduction

One of the most general and aggressive pathologies present in monuments is due to salt crystallization processes [1-11], where damage to rocks is caused by creep-fatigue interaction. The most common salts present in buildings are sulphates, nitrates, phosphates, chlorides, carbonates, etc. The presence of such water soluble salts is usually caused by environmental pollution [12] and groundwater [13] or mobilized from the mortar [14]. All of these aspects should be taken into account in civil engineering studies regarding the restoration and conservation of monuments with historical interest.

One way to avoid the damage caused by the crystallization of water soluble salts is by using non-aggressive methods, such as the application of poultices of sepiolite clay [15-18]. Another possible action is the formation of water-insoluble salts that do not move, thus avoiding creep-fatigue interaction damage caused by the presence of these salts in the rocks [13].

B. Fitzner et al. [19] defined a classification system for pathologies present in monuments, and among these pathologies is the crystallization of soluble salts. In this classification, *B. Fitzner et al.* [19] considers *salt efflorescence* as layers or crystal aggregates of water-soluble salts, whitish and not very consistent, which forms on the surface of porous stone. This occurs due to the migration and evaporation of water containing soluble salts.

* Corresponding author: adolfo.inigo@irnasa.csic.es

Crusts are sheets or shells of coherent material, which are formed on the outside of a rock surface of a transformation product. Its chemical, mineralogical and physical characteristics are partially or completely different from that of stone substrate. Generally crusts develop in layers and are distinguished by their morphological features and hardness.

Disaggregation is the physical alteration that produces material decohesion. This is due to the components of the stone breaking up and falling off. In this case, disaggregation is due to the crystallization of soluble salts, cooling-thawing phenomena and thermal shock. All of these processes are typical of the climate of the area in which the Aqueduct of Segovia is situated (semiarid continental climate with low atmospheric pollution) [5, 20] and are generally accompanied by salt efflorescence visible to the human eye [11].

In this study, we have taken samples of crust, salt efflorescence and disaggregated granite, with or without visible salt efflorescence from the base of different columns of the Aqueduct of Segovia. We analysed ions of the water soluble salts to quantitatively identify the presence of each of these forms of alteration (creep-fatigue interaction between granites and salt solutions in water by capillary).

Materials and methods

The stone material studied, exhibiting granitic pathologies, corresponds to the following varieties: a) Ortigosa del Monte, b) La Granja and c) Magullo. Using XRD, it was determined that all contain the following minerals: a) Quartz, b) Feldspar, c) Plagioclase and d) Micas [21-23]. All have very low porosity, imbibition capacity and a capillary absorption coefficient (Table 1).

Table 1. Hydric properties of quarry samples

Sample	OP	TP	AC	RD	AD	IC	CAC
OQ	1.96	2.39	83	2.65	2.59	0.78	0.000128
GQ	0.74	0.95	79	2.65	2.63	0.30	0.000063
MQ	0.70	0.86	81	2.69	2.66	0.27	0.000052

OP = Open Porosity (%, according to [21]), TP = Total Porosity (%, according to [23]), AC = Absorption Coefficient (%, according to [21]), RD = Reel Density (g/cm^3, according to [23]), AD = Apparent Density (g/cm^3, according to [21]), IC = Imbibition Capacity (%, according to [24]), CAC = Capillary Absorption Coefficient ($g/cm^2s^{0,5}$, according to [23]).
OQ: Ortigosa del Monte quarry; GQ: La Granja quarry; MQ: Magullo quarry.

The Ortigosa del Monte material corresponds to a sienogranite, La Granja to a monzogranite and Magullo to a granodiorite. This classification was made using the results of the chemical analysis of the major elements in the three granites. We classified the three varieties according to the CIPW normative calculation (Q'-ANOR') [25]. Magullo was the variety with the most calcic plagioclases (anorthite) and the Ortigosa del Monte material had the most sodic plagioclases [21].

Sampling was performed on the surface of the granite blocks, and the salts were collected using a brush without damaging the rocks. The crust and salt efflorescence samples were situated on the sides of the columns receiving sunlight, and the disaggregated samples, with or without efflorescence, were on the shaded parts of the columns. The data of the anions and cations are shown in Table 2.

The soluble salts were dissolved in distilled water according to the method used by *A.C. Iñigo et al.* [26]. Once the solutions were prepared, they were quantitatively analysed as follows:

a) Using ion chromatography (instrument: Metrohm 709 IC pump, 732 IC Detector, 733 IC separation centre, suppression module MSM and peristaltic pump Metrohm IC 752), to detect chloride, nitrate, phosphate and sulphate anions.
b) Atomic absorption (instrument: VARIAN SpectrAA FS 3320 - 1475) to detect cations Na^+, K^+, Ca^{2+}, Mg^{2+}, etc.
c) The Calcimeter Bernard Method to detect calcium carbonates.

d) Using the model CON 6/TDS 6 (OAKTON house) we analysed the conductivity of the sample solutions.

Table 2. Chemical composition of the quarry and monument samples selected.

Samples from each group	Atomic absorption (meq/100 g of sample)				Ion chromatography (meq/100 g of sample)				Conductivity (μS)	Calcimeter Bernard Method (%)
	Ca^{2+}	Mg^{2+}	Na^{+}	K^{+}	Cl^{-}	NO_3^{-}	PO_4^{3-}	SO_4^{2-}	Conductivity	$CaCO_3$
OQ	1.39	0.70	0.68	1.04	0.08	0.03	0.19	0.24	13.48	2.02
OQ	1.18	0.60	0.61	1.10	0.07	0.03	0.17	0.23	13.13	2.10
OQ	1.24	0.63	0.65	1.02	0.06	0.02	0.15	0.25	13.28	2.06
GQ	1.74	0.62	0.53	0.97	0.08	0.03	0.03	0.15	13.62	2.00
GQ	1.69	0.69	0.50	0.90	0.07	0.03	0.02	0.12	13.50	1.98
GQ	1.78	0.65	0.55	1.01	0.09	0.02	0.03	0.16	13.70	2.01
MQ	1.12	0.83	0.53	0.92	0.15	0.05	0.05	0.17	12.02	0.00
MQ	1.08	0.80	0.55	0.95	0.12	0.04	0.05	0.16	12.06	0.00
MQ	1.15	0.87	0.52	0.92	0.16	0.05	0.04	0.19	12.03	0.00
C	17.96	7.56	0.30	2.95	0.30	0.35	0.12	0.44	50.17	96.34
C	18.00	11.55	0.59	2.58	0.42	0.96	0.08	15.01	90.23	95.93
C	18.04	15.54	0.88	2.20	0.54	1.57	0.03	25.58	126.29	91.20
C	17.19	11.06	0.56	2.30	0.38	0.93	0.07	13.68	88.90	94.46
E	32.89	420.02	5.36	765.98	5.26	34.97	0.88	538.10	597.95	3.70
E	187.35	123.57	12.45	4.12	5.02	8.07	1.60	370.81	616.77	1.22
E	72.16	141.42	48.53	513.48	9.98	35.89	0.47	295.23	617.00	2.47
E	36.24	610.99	13.33	490.29	6.59	20.59	0.71	799.73	1188.00	7.55
E	46.48	289.07	14.01	1187.96	6.99	17.64	0.22	411.05	791.60	12.40
D	10.27	48.88	7.79	2.61	4.54	11.49	0.09	68.58	212.81	1.64
D	4.76	15.69	4.86	2.42	3.54	6.58	0.56	21.46	88.19	1.81
D	3.91	1.84	3.58	2.88	1.69	3.19	0.73	8.06	47.18	1.19
D	3.91	9.05	2.73	2.57	2.72	5.65	1.06	7.35	54.22	2.04
D	0.94	2.97	5.36	1.63	5.20	6.01	0.36	1.86	38.56	2.35
DE	17.29	9.46	8.94	12.73	4.91	5.09	10.57	21.91	105.81	2.40
DE	21.96	6.18	2.43	5.88	3.05	3.58	0.28	9.37	73.30	5.60
DE	9.98	9.21	14.11	7.91	3.30	6.28	0.20	36.10	119.22	1.22
DE	19.78	7.94	3.32	4.22	2.68	5.25	0.42	38.51	129.71	1.58
DE	17.45	14.53	15.92	32.90	10.62	5.27	41.39	3.65	101.00	1.23
DE	11.68	6.89	5.81	8.46	2.83	3.20	6.90	15.32	78.10	1.80

OQ: Ortigosa del Monte Quarry, GQ: La Granja Quarry, MQ: Magullo Quarry, C: Crust, E: Salt efflorescence, D: Disaggregation, DE: Disaggregation with salt efflorescence.

The Canonical Biplot multivariate method was used in the statistical analysis of the results.

Classical biplot methods [28] allow joint plots of rows and columns of the sample variables within a data matrix in a reduced dimension subspace. There are essentially two types of classical biplots: GH-Biplot = CMP-Biplot (Column Metric Preserving-Biplot), which leads to a high quality for variables, and JK-Biplot = RMP-Biplot (Row Metric Preserving), which leads to a high quality for rows. The results are summarized on several factor planes, where the variables are represented as vectors that start out from a hypothetical origin and the rows as plus (+). If two variables are represented with a very small angle then the variables are highly correlated, if they are opposite their correlation is inverse. Additionally, if the angle is close to perpendicularity, their correlation is minimum. On projecting all the star markers perpendicularly onto the directions of any of the variables, the order of the projections in the direction of those variables is equivalent to the row value on that variable. Nearby star markers are interpreted as similarity and far away star markers as dissimilarity. Several measurements are necessary for a correct Biplot interpretation (Relative Contribution of the Factor to the Element and the Quality of Representation) [29-30].

The Canonical Biplot is a complementary method to MANOVA analysis (Multivariate Analysis of Variance), but it includes all the characteristics of the Biplot method [28], which is aimed at discriminating the set of groups of previously established populations. This technique was later developed and completed by *M.P. Galindo and C. Cuadras* [29], *J.L. Vicente-Villardón* [30] and *I.R. Amaro et al.* [31], and applied to the field of cultural heritage conservation by *M.J. Varas et al.* [32] and *A.C. Iñigo et al.* [33].

Canonical Biplot results are summarized on several factor planes, where the variables are represented as vectors and the means of the different groups as stars (*) surrounded by confidence circles and the matrix rows as plus (+). If two confidence circles are projected perpendicularly on one of the variables and the intervals of both projections do not overlap, this is the same as saying that there are differences between both means (Students' t test); the amplitudes of the circles will depend on the significance, α, determined (MSD, Bonferroni corrections, etc.).

The Canonical Biplot method was applied to a matrix consisting of 29 rows (20 samples from the monument and 9 from de quarries) and 10 columns (Chemical composition ions and conductivity variables). The rows were divided into 7 groups (populations) with specific characteristics:

Quarry granites:	Ortigosa del Monte (OQ), La Granja (GQ) and Magullo (MQ).
Types of pathologies:	Efflorescence (E), Crust (C), Disaggregation (D) and Disaggregation + efflorescence (DE).

Results and discussion

After application of the multivariate Canonical Biplot technique, we obtained a Wilk's lambda of 26.07 ($p < 0.001$), which can be interpreted as though there were differences among the means of the joint measurements of the populations (groups) for all the variables. Regarding the absorption of inertia, the first two axes absorbed 99.89% of the total inertia.

In Figure 1, plane 1-2, we can clearly distinguish the different groups established, and there is a high positive correlation between almost all salts. Only carbonates (perpendicular) and phosphates (low quality representation) are not correlated.

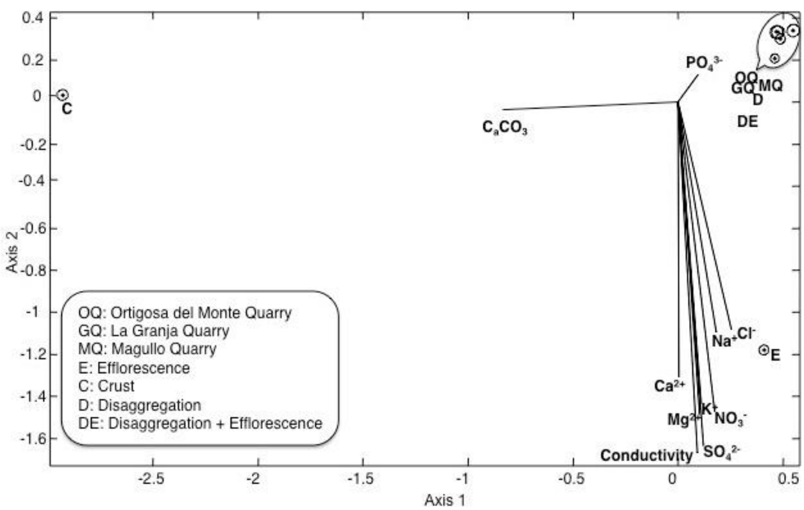

Fig. 1. Canonical Biplot representation on the plane 1-2.

The specific analysis of each group is as follows:

Quarry groups: OQ and GQ are completely overlapping and separated from Magullo MQ. In addition, they are in close proximity and contain very few ions of soluble salts in comparison with monument samples.

Crusts (C): These samples are characterized by large quantity of carbonates (over 90%) and very little of the other salts. In the specific correlations in this group we can see there is an inverse relationship between carbonates and most other salts, for example: SO_4^{2-} (r = -0856), NO_3^- (r = - 0.899), Cl^- (r = - 0.880), Na^+ (r = - .897), Mg^{2+} (r = - 0.897).

This is possibly due to the last restoration carried out on the building, when lime mortar was used for maintenance and reconstruction in some sections and subsequent leakage of the channel through which water flows.

Saline efflorescence (E): These samples are mainly comprised of sulphates and other ions (Cl^-, NO_3^-, Ca^{2+}, Mg^{2+}, K^+ and Na^+) with high conductivity and low concentrations of carbonates.

Disaggregated samples from granites (D): This group overlaps with the group of samples OQ and GQ. This is due to the low content of soluble salts.

Disaggregated samples from granites with salt efflorescence (DE): These are characterized as having a low concentration of soluble salts, but do not contain predominant salts such as sulphates (salt efflorescence) or carbonates (crusts). This occurs because in the dissolving process the weighed sample contains granite minerals, with no soluble salts.

Conductivity data analyses (Table 2) confirmed the above results because samples with a higher content of soluble salts have higher conductivity.

Moreover, we observed there was a high positive correlation between all salts, except for the carbonates that appear perpendicular (near 0 correlations). By contrast, the phosphates showed a negative correlation, but had a low quality of representation Table 3.

Table 3. Correlation matrix for total variables

	Ca^{2+}	Mg^{2+}	Na^+	K^+	Cl^-	NO_3^-	PO_4^{3-}	SO_4^{2-}	Conductivity	$CaCO_3$
Ca^{2+}	1.00	0.35	0.47	0.27	0.44	0.40	0.01	0.54	0.59	-0.01
Mg^{2+}	0.35	1.00	0.35	0.77	0.49	0.75	-0.07	0.98	0.93	-0.09
Na^+	0.47	0.35	1.00	0.46	0.80	0.74	0.22	0.45	0.56	-0.22
K^+	0.27	0.77	0.46	1.00	0.53	0.77	-0.07	0.76	0.77	-0.09
Cl^-	0.44	0.49	0.80	0.53	1.00	0.73	0.53	0.54	0.63	-0.29
NO_3^-	0.40	0.75	0.74	0.77	0.73	1.00	-0.02	0.78	0.78	-0.20
PO_4^{3-}	0.01	-0.07	0.22	-0.07	0.53	-0.02	1.00	-0.09	-0.05	-0.12
SO_4^{2-}	0.54	0.98	0.45	0.76	0.54	0.78	-0.09	1.00	0.97	0.12
Conductivity	0.59	0.93	0.56	0.77	0.63	0.78	-0.05	0.97	1.00	-0.08
$CaCO_3$	-0.01	-0.09	-0.22	-0.09	-0.29	-0.20	-0.12	-0.12	-0.08	1.00

(N = 29)

In this analysis there are two groups (E and C) which are clearly different from the rest. Thus, they were excluded from the analysis in order to obtain a better interpretation.

After application of the multivariate Canonical Biplot in the second analysis, we obtained a Wilk's lambda of 14.56 ($p < 0.001$), where the first two axes absorbed 97.80 % of the total inertia.

In Figure 2 (second analysis, plane 1-2), we observed differences between groups D and DE for all variables ($p < 0.05$). These differences were due to DE presenting higher values than D.

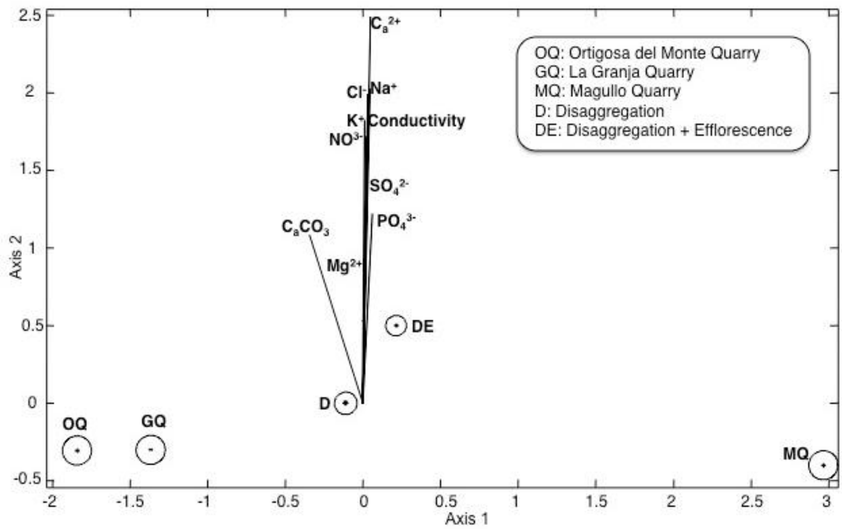

Fig. 2. Canonical Biplot representation on the plane 1-2 without crusts (C) and salt efflorescence (E)

Conclusions

The application of the multivariate Canonical Biplot method to data originating from the chemical analysis of the samples allowed us to make the following conclusions:

a) The composition of water soluble salts and their conductivity can be associated with the type of pathology presented in a building due to creep-fatigue interaction (salt efflorescence, crusts and disaggregation with visible or not salt efflorescence).
b) Sulphate and Cl^-, NO_3^-, Ca^{2+}, Mg^{2+}, K^+ y Na^+ ions are usually the main components of the salt efflorescence, while crusts are made up of carbonate.
c) There are disaggregated granite samples, with or without salt efflorescence, that are intermediate (with fewer soluble salts) between crusts and salt efflorescence.
d) The above conclusions allow us to better diagnose the type of pathology on the monument, which can facilitate future restorations and conservation interventions.

Acknowledgements

The authors are grateful for the funding received from the Town Hall of Segovia, and the National Plan project funded by the Ministry of Education and Science (CGL2007-62168BET and FEDER funds) and Ministry of Science and Innovation (MAT2010-20660)], which permitted this work to be carried out.

References

[1] D. D'Agostino, P. Congedo, R. Cataldo, *Microclimatic assessment and modelling for salt crystallization control in the Crypt of the Duomo of Lecce (South Italy),* **Proceedings of the International Congress on Science and Technology for the Conservation of Cultural Heritage**, 2nd-5th October 2012, Santiago de Compostela, Spain, 2012, pp. 21-24.

[2] T. Rivas-Brea, B. Prieto-Lamas, B. Silva-Hermo, *Artificial weathering of granite*, **Materiales de Construcción**, **58**(289-290), 2008, pp. 179-189.

[3] F.J. Alonso, P. Vázquez, R.M. Esbert, J. Ordaz, *Ornamental granite durability: evaluation of damage caused by salt crystallization test,* **Materiales de Construcción**, **58**(289-290), 2008, pp. 191-201.

[4] J. Ruedrich, S. Siegesmund, *Salt and ice crystallisation in porous sandstones*, **Environmental Geology**, **52**, 2007, pp. 225-249.

[5] A.C. Iñigo, V. Rives, M.A. Vicente, *Reproducción en cámara climática de las formas de alteración más frecuentes detectadas en materiales graníticos, en clima de tendencia continental*, **Materiales de Construcción**, **50**(257), 2000, pp. 57-60.

[6] E. Charola, *Salts in the deterioration of porous materials: An overview*, **Journal of the American Institute for Conservation, 39**(3), 2000, pp. 327-343.

[7] J. García-Talegón, M.A. Vicente, E. Molina, *Decay of granite monuments due to salt crystallization in a non-polluted urban environment*, **Materiales de Construcción**, **49**(253), 1999, pp. 17-27.

[8] M. Robert, E. Bernabé, Ph. Bromblet, A.M. Jaunet, V. Verges-Belmin, M.J. Penven, *Identification of two alteration microsystems chemical and physical, causing granite and kersantite degradation in Brittany (France),* **Proceedings of the EC Workshop on Degradation and Conservation of Granitic Rocks in Monuments**, 28th-30th November 1994, Santiago de Compostela, Spain, 1994, pp. 67-71.

[9] M.A. Vicente, *Granitic materials and historical monuments: study of the factors and mechanisms of weathering and application to historical heritage conservation*, (Summary of Project STEP-CT-90-0101), **Proceedings of the EC Workshop on Degradation and Conservation of Granitic Rocks in Monuments**, 28th-30th November 1994, Santiago de Compostela, Spain, 1994, pp. 4-44.

[10] E. Doehne, *In situ dynamics of sodium sulphate hydration and dehydration, in stones pores: observations at high magnification using the environmental scanning electron microscope*, **Proceedings of the 3rd International Symposium on The Conservation of Monuments in the Mediterranean Basin**, 22th-25th June 1994, Venice, Italy, 1994, pp. 143-150.

[11] M. El Khalili, *Damage assessment of the Roman Nymphaeum in Amman, Jordan: An analytical and diagnostic study,* **International Journal of Conservation Science, 7**(2), 2016, pp. 477-492.

[12] C. Saiz-Jimenez, P. Brimblecombe, D. Camuffo, R.A. Lefèvre, R. Van Grieken, *Damages caused to European monuments by air pollution: assessment and preventive measures*, **Proceedings of the International Workshop on Air Pollution and Cultural Heritage**, 1st-3rd December 2003, Seville, Spain, 2003, pp. 91-109.

[13] A. Arnold, *Altération et conservation d'oeuvres culturelles en matériaux poreux affectés par des sels*, **Procedings of 7es Journées d'Etudes de la SFIIC on Le Dessalement des Matériaux Poreux**, 9th-10th May 1996, Poitiers, France, 1996, pp. 3-20.

[14] P.F. O'Brien, E. Bell, S. Pavia-Santamaria, P. Boyland, T.P. Cooper, *Role of mortars in the decay of granite*, **Science of the Total Environment**, **167**, 1995, pp. 103-110.

[15] J. García-Talegón, A.C. Iñigo, V. Vicente-Palacios, *A laboratory simulation of desalting on calcareous building stone with wet sepiolite*, **Environmental Earth Sciences**, **75**, 2016, pp. 925-932.

[16] M.I. Carretero, J.M. Bernabé, E. Galán, *Application of sepiolite-cellulose pastes for the removal of salts from building stones*, **Applied Clay Science**, **33**, 2006, pp. 43-51.

[17] M.A. Vicente, S. Vicente-Tavera, *Clay poultices in salt extraction from ornamental stones: A statistical approach*, **Clays and Clay Minerals**, **49**(3), 2001, pp. 227-235.

[18] R. Trujillano, J. García-Talegón, A.C. Iñigo, M.A. Vicente, V. Rives, E. Molina, *Removal of salts from granite by sepiolite*, **Applied Clay Science, 9**, 1995, pp. 459-463.

[19] B. Fitzner, K. Heinrichs, R. Kownatzki, *Classification and mapping of weathering forms*, **Proceedings of 7th International Congress on Deterioration and Conservation of Stone,** 15th-18th June 1992, Lisbon, Portugal, 1992, pp. 957-968.
[20] J. García-Talegón, M. González-Sánchez, A.C. Iñigo, S. Vicente-Tavera, V. Rives, *Microenvironments in the inner and outer of the Zamora Cathedral*, **Proceedings of the International Conference on Heritage, Weathering and Conservation**, **1**, 21th-24th June 2006, Madrid, Spain, 2006, pp. 457-461.
[21] A.C. Iñigo, J. García-Talegón, S. Vicente-Tavera, S. Martín-González, S. Casado-Marín, J.L. Pérez-Rodríguez, M. Vargas-Muñoz, *Colour and ultrasound propagation speed changes by different ageing of freezing/thawing and cooling/heating in granitic materials*, **Cold Region Science and Technology**, **85**, 2013, pp. 71-78.
[22] D. Grossi, E.A. del Lama, J. Garcia-Talegon, A.C. Iñigo, S. Vicente-Tavera, *Evaluation of colorimetric changes in the itaquera granite of the Ramos de Azevedo Monument, São Paulo, Brazil,* **International Journal of Conservation Science, 6**(3), 2015, pp. 313-322.
[23] V. Pelin, I. Sandu, S. Gurlui, M. Branzila, V. Vasilache, E. Bors, I.G. Sandu, *Preliminary investigation of various old geomaterials treated with hydrophobic pellicle*, **Color Research and Application, 41**(3), Special Issue: SI, 2016, pp. 317-320.
[24] A.C. Iñigo, S. Vicente-Tavera, V. Rives, *Statistical design applied to hydric property behaviour for monitoring granite consolidation and/or water-repellent treatments*, **Materiales de Construcción**, **56**(281), 2006, pp. 17-28.
[25] A.C. Iñigo, S. Vicente-Tavera, V. Rives, M.A. Vicente, *Porosidad libre en granitos alterados: Comentarios a las normas*, **Materiales de Construcción**, **45**(238), 1995, pp. 47-53.
[26] A. Streckeisen, R.W. Le Maitre, *Neues Jahrbuch für Mineralogie*, **Abhandlungen, 136**, 1979, pp. 169-206.
[27] A.C. Iñigo, R. Alonso, S. Vicente-Tavera, *Dissolution of salts crystallised in building materials using ultrasound: an alternative to the NORMAL (1983) normative*, **Ultrasonic Sonochemistry, 8**, 2001, pp. 127-130.
[28] K.R. Gabriel, *Goodness of fit of biplots and correspondence analysis*, **Biometrika**, **89**(2), 2002, pp. 423-436.
[29] M.P. Galindo, C. Cuadras, *Una alternativa de representación simultanea: HJ-Biplot*, **Qüestiió**, **1**, 1986, pp. 13-23.
[30] J.L. Vicente-Villardón, **MULTBIPLOT**: **Multivariate Analysis using Biplots**, http://biplot.usal.es. [accessed on Mar 26, 2016].
[31] I.R. Amaro, J.L. Vicente-Villardón, M.P. Galindo-Villardón, *ANOVA Biplot para arreglos de tratamientos con dos factores basado en modelos lineales generales multivariantes*, **Interciencia**, **29**, 2004, pp. 26-32.
[32] M.J. Varas, S. Vicente-Tavera, E. Molina, J.L. Vicente-Villardón, *Role of canonical biplot meted in the study of building stones: an example from Spanish monumental heritage*, **Environmetrics**, **16**, 2005, pp. 1-15.
[33] A.C. Iñigo, J. García-Talegón, S. Vicente-Tavera, *Canonical Biplot statistical analysis to detect the magnitude of the effects of phosphates crystallization aging on the color in siliceous conglomerates*, **Color Research and Application**, **39**(1), 2014, pp. 82-87.

Received: June 23, 2016
Accepted: February 19, 2017